



Monitoring Endocytic Trafficking of Anthrax Lethal Factor by Precise and Quantitative Protein Labeling**

Siqi Zheng, Gong Zhang, Jie Li, and Peng R. Chen*

Abstract: Coupling the genetic code expansion technique with bioorthogonal reactions enables precise control over the conjugation site as well as the choice of fluorescent probes during protein labeling. However, the advantages of this strategy over bulky and rigid fluorescent proteins (FPs) remain to be fully explored. Here we applied site-specific bioorthogonal labeling on anthrax lethal factor (LF) to visualize its membrane translocation inside live cells. In contrast to the previously reported FP tags that significantly perturbed LF's membrane trafficking, our precisely and quantitatively labeled LF exhibited an endocytic activity comparable to wild-type LF. This allowed time-lapse imaging of LF's natural translocation process from host cell membrane to cytosol, which revealed molecular details of its virulence mechanism. Our strategy is generally applicable for monitoring intracellular protein membrane translocation that is difficult to access using conventional protein labeling methodologies.

Fluorescence proteins (FPs) have revolutionized our ability to visualize and monitor proteins in living systems.^[1] Still, the applications of FPs are hindered in many circumstances. One major drawback is their bulky size, which, in conjunction with the largely confined fusion sites at protein's N- or C-terminus, may cause significant perturbations to the structure and/or function of the native protein. In addition, the low photophysical property as well as the propensity for photobleaching further restricted the utilization of these FP tags. To circumvent these limitations, several alternative protein labeling techniques have emerged in recent years.^[2] Among them, coupling the genetic-code expansion strategy with bioorthogonal reactions offers a facile and powerful approach for

labeling proteins with increased precision and lowered perturbation. Indeed, by site-specific incorporation of a bioorthogonal handle, typically in the form of unnatural amino acids (UAAs), into the protein of interest, this method allows the subsequent bioorthogonal labeling of the protein with a small-molecule fluorophore at virtually any desired residue.^[3] Therefore, a wide spectrum of organic dyes with various photophysical properties can be chosen as the labeling probe while the labeling site can be precisely controlled to minimize potential perturbations to proteins. Moreover, multiple highly efficient bioorthogonal reactions are currently available for producing homogeneously labeled protein samples that is another critical determinant for imaging intracellular protein trafficking. Nevertheless, the value of this "precise and quantitative" protein labeling strategy in a real biology setting, particularly its advantages over conventional labeling methods including FP tags, remains to be fully demonstrated.

Monitoring protein intracellular translocation is a prominent example where a precise protein labeling technique is highly desired. The translocation of proteins across cellular membrane is a complicated process that requires a series of precisely regulated mechanism.^[4] In particular, the labeling strategy needs to be compatible with protein's unfolding and refolding processes before and after the membrane translocation. Even some trivial perturbation to the protein cargo's structure or function may abandon its translocation activity. Therefore, imaging such fundamental processes, particularly the time-course study on live cells, is extremely challenging. Here we chose to label and monitor the cellular entry process of Anthrax lethal factor (LF), a highly virulent protein known to travel through both cell membrane and the endosomal membrane to establish infection within host cytosol (Scheme 1).^[5]

The notoriously known bacterial toxin LF is a zinc-dependent protease capable of cleaving the canonical substrates mitogen-activated protein kinase kinases (MEKs) as well as Nod-like Receptor family, pyrin domain containing 1b (Nalp1b)^[6] through receptor-mediated endocytosis with anthrax protective antigen (PA).^[7] leading to the disruption of a wide range of downstream signaling pathways that cause the immediate death of host immune cells such as macrophage.^[8] Previous work showed that translocation of LF through cell membrane requires the binding of LF to the membrane-anchored active form of PA (PA₆₃) heptamer and the LF-PA complex undergoes the clathrin-mediated endocytosis to reach cell endosome.^[9] Once in late endosome, the decreased pH induces the insertion of a unique α -helix on PA pore to form a narrow channel through endosome membrane.^[10] LF then adopts a pH-triggered partial unfolding to

[*] S. Zheng,^[‡] J. Li, Prof. Dr. P. R. Chen

Beijing National Laboratory for Molecular Sciences, Key Laboratory of Bioorganic Chemistry and Molecular Engineering of Ministry of Education, Synthetic and Functional Biomolecules Center, College of Chemistry and Molecular Engineering, Peking University Beijing 100871 (China)

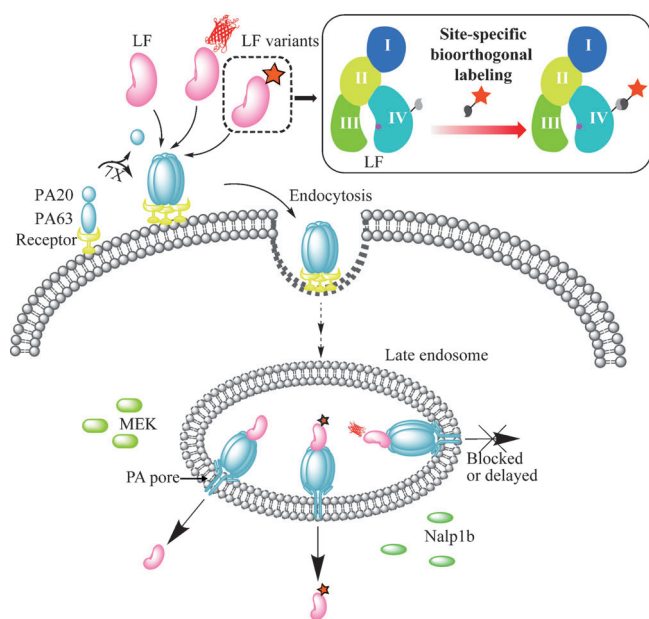
E-mail: pengchen@pku.edu.cn

G. Zhang,^[‡] Prof. Dr. P. R. Chen
Peking-Tsinghua Center for Life Sciences
Beijing (China)

[‡] These authors contributed equally to this work.

[**] We thank Prof. Feng Shao (NIBS, China) for donation of plasmids and Dr. Rong Meng (Peking University, China) for MS detection. This work was supported by the National Basic Research Program of China (2010CB912302 and 2012CB917301) and the National Natural Science Foundation of China (21225206 and 91313301).

Supporting information for this article is available on the WWW under <http://dx.doi.org/10.1002/ange.201403945>.



Scheme 1. Monitoring the internalization process of LF from host cell surface into the cytosol using a “precise” site-specific bioorthogonal protein labeling strategy.

pass through this narrow channel and refolds within host cytosol.^[11] The efficient translocation of full-length LF from late endosome to cytosol is critical for establishing its virulence effects inside host cells. Although LF’s translocation through PA pore has been chemically dissected in vitro,^[12] this translocation process has not been directly visualized within live cells. Time-lapse imaging of the entire cellular entry process by fluorescent labeled LF would illustrate the molecular details underlying its endocytic trafficking.

The proper function of LF depends on the delicate coordination among its four domains: the N-terminal domain I is the PA recognition domain that is crucial for its cell entry; domain II and III are the substrates recognition domains that form a groove capable of docking the MEK substrates; and domain IV contains the zinc-binding protease site while several residues in domain III also support the proteolytic activity of LF (Figure 1A).^[13] Introducing GFP to the N-terminus of LF or the modification of residues within domain I would disrupt its endocytic activity, whereas the C-terminal fusion of FP tags has been shown to significantly delay or even block its passing through the endosomal membrane.^[14] Meanwhile, since many native residues on LF such as lysines are involved in PA recognition or substrate interaction, labeling through these natural residues may result in a non-uniform distribution of labeled LF and would also interfere with its cellular entry or substrate cleavage.^[15] Finally, adding a cysteine residue to LF can potentially generate disulfide bridges or unwanted aggregates. To circumvent these issues, we performed site-specific labeling of LF via a genetically encoded bioorthogonal handle and the corresponding bioorthogonal reaction. We envisioned that the small-sized fluorophore and the optimized labeling site and procedure may cause negligible interruption to LF’s function, particularly its membrane translocation activity, upon entering cells.

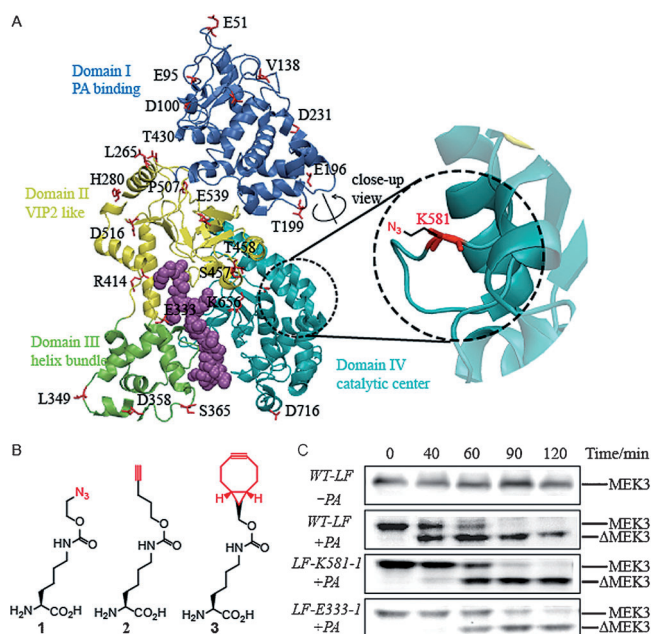


Figure 1. Site-specific incorporation of bioorthogonal handle-bearing UAAs into LF. A) The crystal structure of LF (PDB 1JKY) with its substrate MAPKK2 and its four domains differently colored and the UAA incorporation sites labeled. B) Structures of Pyl analogues bearing different bioorthogonal handles utilized in this study. C) The azide-bearing LF variants did not cause interruption of its protease activity on MEK substrates.

We started by finding a suitable labeling reaction on LF. The presence of transition metal ions such as Cu^I or Pd^{II} both caused the loss of LF’s enzymatic activity, likely due to the disruption of the fragile structure of LF. In contrast, LF’s activity remained unaffected in the presence of DBCO(dibenzocyclooctyne)-Fluor 545 or FITC(fluorescein isothiocyanate)-tetrazine, the reagents utilized for strain-promoted azide–alkyne cycloaddition (SPAAC) or inverse-electron-demand Diels–Alder (IEDDA) reactions, respectively (Figure S1 in the Supporting Information). Therefore, we focused on these metal-free bioorthogonal reactions. The pyrrolysine-based genetic code expansion system was first used to introduce several bioorthogonal handles participating in these reactions onto LF.^[16] Western blotting against the C-terminal His-tag showed that LF variants containing azido- or alkynyl-Pyl analogues (**1** and **2**) were expressed in a much higher yield than that containing the Pyl analogue bearing a BCN (bicyclo[6.1.0]nonyne, **3**) moiety (Figure S2).^[2b, 16b, 17] This is likely due to the large size of the cyclooctyne ring on BCN, which may suggest that direct incorporation of bulky fluorescent UAAs such as Anap (3-(6-acetylnaphthalen-2-ylamino)-2-aminopropanoic acid) could also significantly disrupt LF’s folding. Taken together, our results showed that SPAAC-mediated ligation between **1** and DBCO-Fluor 545 offered a non-invasive strategy suitable for site-specific labeling of LF.

Next we screened the UAA-incorporation site on LF in order to obtain a fluorescent labeled variant with a high labeling yield and near wild-type activity. The entire labeling process was kept at 4 °C to avoid LF denaturation at a higher

temperature. A total of 25 residues throughout LF's four domains were examined and approximately half of these sites showed a relatively high expression level in the presence of **1** (Figure S3). We also confirmed that incorporation of **1** at a single site did not alter the native folding or function of LF (Figure 1 C). The SPAAC-mediated fluorescent labeling was then applied to LF variants bearing the site-specifically incorporated azide handle. Among the total of 25 sites we inspected, five LF variants showed acceptable protein expression level and fluorescent labeling efficiency as judged by the relative fluorescence ratio (Figure S4 and also see calculation in the Supplementary Method 6).

We then compared the enzymatic activity of these five fluorescent LF variants with that of wild-type LF (WT-LF) and FP-fused LF in vitro and in vivo. Interestingly, whereas a similar cleavage rate was detected for all LF variants we examined on MEK1, their proteolytic activity inside living cells were significantly altered (Figure 2A,B and S5). For example, the MEK cleavage rate reached 70 % within 120 min for WT-LF upon interacting with cell membrane. In contrast, LF-EGFP showed markedly delayed MEK cleavage while LF-mCherry's protease activity was almost completely abandoned within the time we tested (≈ 120 min). Our five fluorescent labeled LF variants also showed varied MEK cleavage rates, with the labeling site at a surface exposed residue K581 possessing a time-dependent enzymatic activity

essentially at the same level with that of WT-LF. These results indicated that neither FP tags nor the site-specifically labeled fluorophores affected the enzymatic activity of LF in vitro. However, these modifications may decrease the unfolding and/or refolding efficiency of LF in vivo. In particular, LF's passing through the PA channel on endosomal membrane may be hindered, resulting in delayed or blocked membrane translocation. Indeed, previous study showed that the large energy requirement within the unfolding process of FPs could perturb the transmembrane efficiency of LF-EGFP and LF-mCherry proteins.^[14] These results further strengthened the rational in screening multiple labeling residues on the same protein in order to obtain an optimal labeling site without the loss of protein's native activity in vivo. Therefore, we focused on labeling LF through residue K581 for further study and this DBCO-Fluor 545 labeled LF variant was renamed LF-K581-Fluo545. LC-MS/MS analysis confirmed the specific and quantitative conjugation between DBCO-Fluor 545 and **1** at residue 581 on LF (the efficiency reached 99 % after 6 h incubation at 4 °C; Figure 2C, S4D and S6).

More detailed time-course comparison on the activity between LF-K581-Fluo545 and WT-LF was next carried out. WT-LF started to cleave MEK3 as early as 25 min after mixing with PA. To our delight, LF-K581-Fluo545 exhibited a similarly MEK cleavage rate at this early time point (Figure S7). Furthermore, we compared the cleavage efficiency at 60 min because nearly half of MEK3 was found to be hydrolyzed by WT-LF at this time point. LF-K581-Fluo545's hydrolysis activity on MEK3 was found to be synchronous with WT-LF at 60 min (Figure 2D). Finally, the toxicity analysis towards macrophages J774A.1 cells showed that LF-K581-Fluo545 exhibited a similar lethal effect on this cell type as WT-LF at a wide range of concentrations (Figure 2E). Taken together, these results demonstrated that unlike FP tags, our site-specifically labeled LF variant LF-K581-Fluo545 did not interfere with its membrane translocation capability. The time-lapse imaging of LF's natural endocytic process on living cells may thus become possible.

Finally, we applied LF-K581-Fluo545 for time-lapse imaging of LF's internalization and translocation on live cells (Figure 3). We proposed that the time dependent localization of LF-K581-Fluo545, rather than LF-EGFP or LF-mCherry, could convincingly represent the native translocation time-course of LF. Notably, consistent with the aforementioned enzymatic activity results, LF-mCherry remained within the late endosome of BHK-21 cells 30 min after toxin delivery as indicated by co-localization with a late endosome marker Rab7 (Figure S8). In fact, LF-mCherry remained completely trapped in acidic cellular compartments, probably late endosome or lysosome, and co-localized with LysoTracker during our imaging experiments up to 120 min (Figure S9). Similarly, LF-EGFP co-localized with Rab7 without detectable dispersion out of endosome at 30 min (Figure S10). In contrast, a considerable portion of LF-K581-Fluo545 was found to translocate through endosomal membrane and disperse into cytosol within 20 min after toxin delivery. Although internalization efficiency slightly varies between cells, this observation indicated a rather fast cell entry process of the exogenously delivered toxin such as LF,

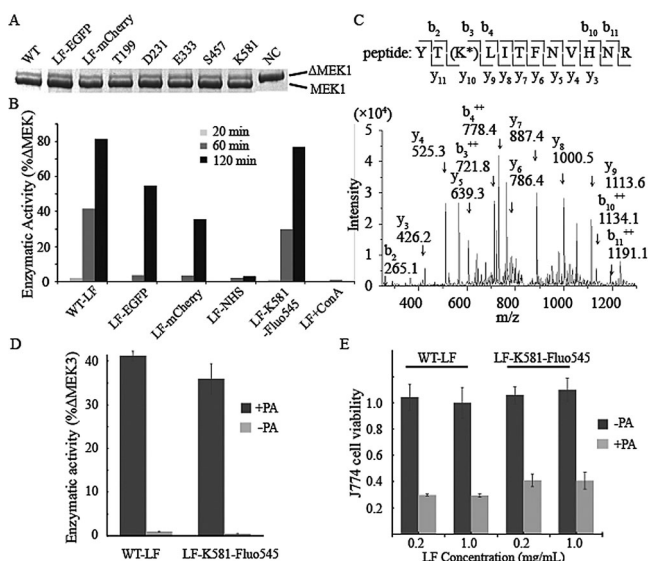


Figure 2. Labeling efficiency and enzymatic activity of fluorescent labeled LF variants. A) Enzymatic activity of LF variants in vitro measured by cleavage of its substrate MEK1. Band on the top: full length MEK1; band below: cleavage product. B) Enzymatic activity of LF variants in vivo calculated by quantification of the normalized ratio of cleaved MEK3 (Δ MEK3) to total MEK3. LF-NHS: Cy3-NHS labeled LF; ConA: Concanamycin A. C) LC-MS/MS analysis of fluorescent labeled LF variant LF-K581-Fluo545. K* represents DBCO-Fluor 545 labeled UAA 1. D) The enzymatic activity of WT-LF and LF-K581-Fluo545 variants at 60 min determined by cleavage of MEK3. Error bars from three independent experiments. E) LF-K581-Fluo545 induced apoptosis in J774A.1 cells in a pattern similar to WT-LF. Cell viability determined by MTS assay, error bars from three independent experiments.

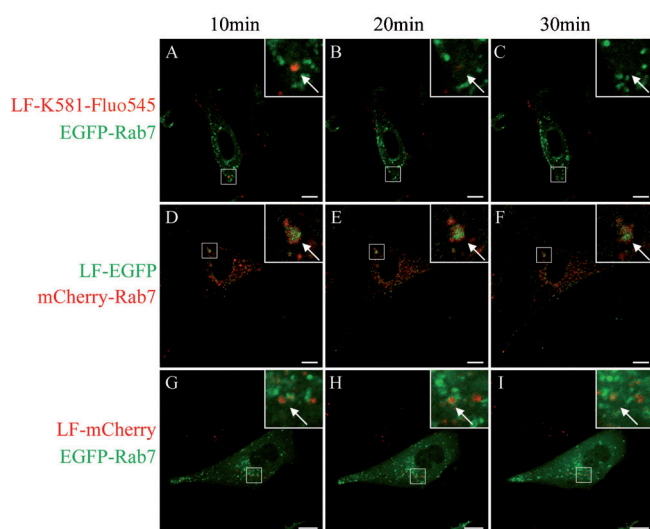


Figure 3. Translocation time-course of different LF variants. The red and green channels represent the corresponding proteins shown on the left. Time points are indicated on top. A–C) Majority of LF-K581-Fluo545 translocated into cytosol within 30 min. D–F) Most LF-EGFP was located in late endosome after 30 min. G–I) LF-mCherry was completely trapped within endosome after 30 min. Scale bars: 10 μ m.

which agreed well with our measured time scale on LF's MEK cleavage activity that should immediately follow its translocation through the endosomal membrane (≈ 20 min after delivery; Figure S7, S11, S12 and S13). Interestingly, although LF-K581-Fluo545 was fully capable of travelling through endosomal membrane, we found that a reservoir of LF-K581-Fluo545 was constantly located inside the acidic cellular compartments within the time-course we measured (up to 120 min; Figure S9). This observation implied that late endosome may slowly release LF into cell cytosol and this intracellular translocation is a highly heterogeneous process. In consistent with this hypothesis, previous study demonstrated that the cytosol-residing LF can be degraded by the host ubiquitination pathway with a half-life of approximately 3 h and LF needs to be shielded from cytosol for long term efficacy.^[18] Therefore, our observation may provide a direct evidence supporting the highly heterogeneous nature of LF's endosomal release during its internalization. Considering multiple proteolysis systems exist inside mammalian cells to degrade exogenous proteins including bacterial toxins, the prolonged maintenance and slow release of LF from intraluminal vesicles may account for the underlying mechanism of the continuous toxicity up to several days after anthrax infection. The acidic cellular compartments of fibroblasts (BHK-21 cells) might serve as a buffering source for LF toxicity. Finally, in order to further verify the reliability of our observations, we also treated cells with Concanamycin A (ConA) which can prevent the pore-formation of PA and thus block LF's escape from endosome.^[19] As expected, LF-K581-Fluo545 was completely blocked in the Rab7 containing vesicles under this circumstance, which was also in agreement with our measured enzymatic activity (Figure S14).

In summary, by using a highly efficient bioorthogonal reaction between a site-specifically incorporated UAA handle and a small molecule fluorephore, we have precisely and quantitatively labeled anthrax LF, which enabled the time-lapse monitoring of its internalization and membrane translocation processes within live cells. To our knowledge, our study represents the first report that the time-course for LF's natural endocytosis process was directly visualized and measured, which revealed a slow endosomal release mechanism that may protect bacterial toxin from protein degradation machinery inside host cells. The wide applicability of bioorthogonal reactions and genetic-code expansion technique would make our method readily adaptable for investigating the membrane translocation process of additional bacterial virulence effectors, as well as many other types of proteins when the bulky size and/or rigid nature of FP tags become an issue. Finally, recent study suggested that the cyclooctyne type of molecules may undergo side reactions with cellular nucleophiles and thus cause high backgrounds for live cell labeling.^[20] Our work here showed that such strain-promoted cycloaddition reactions cause much lower perturbations on intact proteins than transition metal-catalyzed reactions, which should be useful for in vitro labeling of proteins containing delicate structures and multiple functional domains.

Received: April 2, 2014

Published online: May 14, 2014

Keywords: anthrax lethal factor · bioorthogonal reactions · genetic code expansion · membrane translocation · protein labeling

- [1] M. Chalfie, Y. Tu, G. Euskirchen, W. W. Ward, D. C. Prasher, *Science* **1994**, 263, 802–805.
- [2] a) M. W. Popp, J. M. Antos, G. M. Grotenbreg, E. Spooner, H. L. Ploegh, *Nat. Chem. Biol.* **2007**, 3, 707–708; b) D. P. Nguyen, H. Lusic, H. Neumann, P. B. Kapadnis, A. Deiters, J. W. Chin, *J. Am. Chem. Soc.* **2009**, 131, 8720–8721.
- [3] a) L. Davis, J. W. Chin, *Nat. Rev. Mol. Cell Biol.* **2012**, 13, 168–182; b) M. Grammel, H. C. Hang, *Nat. Chem. Biol.* **2013**, 9, 475–484.
- [4] W. Wickner, R. Schekman, *Science* **2005**, 310, 1452–1456.
- [5] R. J. Collier, J. A. Young, *Annu. Rev. Cell Dev. Biol.* **2003**, 19, 45–70.
- [6] J. L. Levinsohn, Z. L. Newman, K. A. Hellmich, R. Fattah, M. A. Getz, S. Liu, I. Sastalla, S. H. Leppla, M. Moayeri, *PLoS Pathog.* **2012**, 8, e1002638.
- [7] a) C. Montecucco, F. Tonello, G. Zanotti, *Trends Biochem. Sci.* **2004**, 29, 282–285; b) B. A. Krantz, R. A. Melnyk, S. Zhang, S. J. Juris, D. B. Lacy, Z. Y. Wu, A. Finkelstein, R. J. Collier, *Science* **2005**, 309, 777–781.
- [8] a) G. L. Johnson, R. Lapadat, *Science* **2002**, 298, 1911–1912; b) J. M. Park, F. R. Greten, Z. W. Li, M. Karin, *Science* **2002**, 297, 2048–2051.
- [9] J. A. Young, R. J. Collier, *Annu. Rev. Biochem.* **2007**, 76, 243–265.
- [10] a) E. Santelli, L. A. Bankston, S. H. Leppla, R. C. Liddington, *Nature* **2004**, 430, 905–908; b) K. L. Thoren, B. A. Krantz, *Mol. Microbiol.* **2011**, 80, 588–595.
- [11] a) L. Abrami, N. Reig, F. G. van der Goot, *Trends Microbiol.* **2005**, 13, 72–78; b) K. L. Thoren, E. J. Worden, J. M. Yassif,

- B. A. Krantz, *Proc. Natl. Acad. Sci. USA* **2009**, *106*, 21555–21560.
- [12] a) S. Zhang, E. Udho, Z. Wu, R. J. Collier, A. Finkelstein, *Biophys. J.* **2004**, *87*, 3842–3849; b) B. L. Pentelute, O. Sharma, R. J. Collier, *Angew. Chem.* **2011**, *123*, 2342–2344; *Angew. Chem. Int. Ed.* **2011**, *50*, 2294–2296.
- [13] A. D. Pannifer, T. Y. Wong, R. Schwarzenbacher, M. Renatus, C. Petosa, J. Bienkowska, D. B. Lacy, R. J. Collier, S. Park, S. H. Leppla, P. Hanna, R. C. Liddington, *Nature* **2001**, *414*, 229–233.
- [14] I. Zorretta, L. Brandi, B. Janowiak, F. Dal Molin, F. Tonello, R. J. Collier, C. Montecucco, *Cell. Microbiol.* **2010**, *12*, 1435–1445.
- [15] G. A. Dalkas, A. Papakyriakou, A. Vlamis-Gardikas, G. A. Spyroulias, *Protein Sci.* **2009**, *18*, 1774–1785.
- [16] a) N. J. Agard, J. A. Prescher, C. R. Bertozzi, *J. Am. Chem. Soc.* **2004**, *126*, 15046–15047; b) K. Lang, L. Davis, S. Wallace, M. Mahesh, D. J. Cox, M. L. Blackman, J. M. Fox, J. W. Chin, *J. Am. Chem. Soc.* **2012**, *134*, 10317–10320.
- [17] J. Li, S. Lin, J. Wang, S. Jia, M. Yang, Z. Hao, X. Zhang, P. R. Chen, *J. Am. Chem. Soc.* **2013**, *135*, 7330–7338.
- [18] L. Abrami, L. Brandi, M. Moayeri, M. J. Brown, B. A. Krantz, S. H. Leppla, F. G. van der Goot, *Cell Rep.* **2013**, *5*, 986–996.
- [19] M. Huss, G. Ingenhorst, S. König, M. Gassel, S. Droese, A. Zeeck, K. Altendorf, H. Wiczorek, *J. Biol. Chem.* **2002**, *277*, 40544–40548.
- [20] K. E. Beatty, J. D. Fisk, B. P. Smart, Y. Y. Lu, J. Szychowski, M. J. Hangauer, J. M. Baskin, C. R. Bertozzi, D. A. Tirrell, *Chem-BioChem* **2010**, *11*, 2092–2095.